Design and Flight Test of a Kevlar Acoustic Liner

Harold C Lester,* John S Preisser,† and Tony L Parrott*
NASA Langley Research Center, Hampton, Virginia

This paper summarizes the design, fabrication, and flight evaluation of a Kevlar acoustic liner for a JT15D turbofan engine The liner was designed to suppress by a measurable amount a dominant (13,0) BPF tone This tone or spinning mode was produced for research purposes by installing 41 circumferentially distributed small diameter rods upstream of the 28 fan blades Duct liner attenuations calculated by a finite element procedure are compared to far field power (insertion) losses deduced from flight data The finite element program modeled the variable geometry of the JT15D inlet and used a uniform flow with a boundary layer roll off to model the inlet flowfield Measured far field power losses were generally greater than attenuations calculated by the finite element computer program

Nomenclature

a	= outer radius at fan face
c_0	= speed of sound
d	= liner depth
f	= frequency
j	$=\sqrt{-1}$
k	= free space wave number, ω/c_0
M_f	= Mach number at fan face
$(m\ n)$	= (circumferential, radial) mode numbers where (0,0) denotes plane wave
SPL	= sound pressure level
t	= time, $e^{-j\omega t}$ time convention
x	= axial coordinate
β	= acoustic admittance ratio, $\beta_R + j\beta_I = \zeta^{-1}$
γ	= wave number
ζ	= acoustic impedance ratio (normalized by characteristic impedance of air) $\theta + j\chi$
ζ_c	= characteristic acoustic impedance ratio of bulk material
ζ_f	= acoustic impedance ratio due to facesheet
ζ_i	= acoustic impedance ratio due to interaction of bulk material and facesheet
ζ_n	= acoustic impedance ratio due to nonlinear effects
θ	= acoustic resistance ratio
ξ	= cut off ratio
χ	= acoustic reactance ratio (note: $e^{-j\omega t}$ time con vention)
ω	$=2\pi f$

Introduction

DURING the last several years a NASA intercenter research program has been underway to develop and evaluate techniques for simulating in flight fan noise by means of wind tunnel and static ground tests of turbofan engines [1 3] The flight test portion of the program was con ducted using a JT15D turbofan engine mounted under the starboard wing of an OV 1B Mohawk aircraft During the latter phases of this flight program, an opportunity arose to design construct, and flight test a Kevlar acoustic liner configuration The purpose of this paper is to evaluate the liner design analysis by comparison of calculated liner per formance with far field power losses deduced from flight data

The liner design objective was to suppress a dominant blade passage frequency (BPF) tone by a measurable amount This tone was generated for research purposes by installing 41 circumferentially-distributed small diameter rods upstream of the 28 fan blades [1] The resulting interaction between the rod wakes and the fan blades produced a (13,0) acoustic spinning mode at the blade passage frequency Translation of the liner design into flight hardware was achieved by constructing the liner so that its impedance properties at selected frequencies were as close as possible to design target values in the operational range of interest—about 3 7 to 4 9 kHz These target impedance values were based on calculations from a finite element computer program[4] which modeled the propagation of sound through the variable geometry and internal flow of the JT15D inlet To cover the operational frequency range of the flight tests, a bulk absorber type liner was thought to be more appropriate than a tuned or resonant liner configuration Kevlar was chosen as the bulk liner material [5 7]

The flight tests were conducted at NASA's Wallops Flight Facility. Details describing the flight tests, instrumentation, and data reduction procedures of similar (without rods) OV 1B/JT15D configurations are given in Ref 3 To evaluate the liner performance, far field acoustic pressure measurements were recorded and analyzed Liner attenuations calculated by the finite element computer program were evaluated on the basis of far field BPF directivity and power loss data reduced from the flight measurements

Flight Configuration and Tests

In this section the OV 1B/JT15D flight configuration and data reduction systems are reviewed This is followed by a discussion of the liner test objective

Flight Configuration

The flight configuration shown in Fig 1 consisted of an OV 1B aircraft with a JT15D turbofan engine mounted under its starboard wing As reported in Ref 3, this setup was used extensively as part of NASA's Flight Effects Program All

Presented as Paper 83 0781 at the AIAA 8th Aeroacoustics Con ference Atlanta Ga , April 11 14, 1983; received Aug 8 1983; revision received Jan 6, 1984

*Aerospace Engineer
†Aerospace Engineer Member AIAA

flight tests were performed with the starboard turboprop engine shut down and feathered in order to avoid any extraneous noise from ingestion of the prop wake into the test engine As shown in Fig 2, the JT15D engine was modified in two ways for the tests discussed in this paper First a circumferential array of 41 small diameter cylindrical rods was secured to the wall just forward of the fan, and second an acoustic liner was installed over the full circumference of the interior duct wall

A schematic of the JT15D inlet is shown in Fig 3 A similar assembly of 41 rods had been tested previously[1] in a hardwall JT15D/inlet assembly mounted on a static test stand The rods used were 3/16 in diam stainless steel and protruded 2 5 in from the wall into the duct The rods were mounted about 3 in in front of the leading edge of the fan blades and were equally spaced circumferentially around the interior duct wall

The inlet duct, as illustrated approximately to scale in Fig 3 is nearly cylindrical varying from a diameter of 19 9 in at the throat ($x=1$ 05) to 21 0 in in the liner region The aft edge of the liner is about 6 in in front of the fan face and extends forward approximately 9 6 in to cover the back half of the interior duct wall The liner was partitioned axially into four equal length sections of about 2 4 in each Because of the centerbody location, the two aft liner sections are located in an annular cross section, whereas the two forward liner sections exist in a circular duct section

During the flight tests aluminum tape was used to cover various axial sections of the liner in order to simulate a hardwall boundary condition In this manner the effect of liner length was studied over a wide fan speed (frequency) range of the JT15D engine

Data Systems

The JT15D/OV 1B flight tests made extensive use of several data measuring systems [2,3] Engine performance and aircraft state parameters were recorded by tape recorders on the aircraft The far field acoustic data were recorded by a linear array of eight 0 5 in condensor type free field microphones mounted on 30 ft poles and placed directly under the flight path [3] In conjunction with laser radar tracking information and weather profile data, the acoustic data were ensembled averaged and adjusted to a static equivalent, lossless atmospheric condition at a constant radius of 100 ft Such a normalization procedure allowed data sets recorded on different days under varying conditions to be compared directly Further description of the flight tests and data processing techniques can be found in Ref 3

Test Objectives

The objective of the test program was to validate with flight data the design methodology described in this paper In this respect it was mandatory to avoid eliminating the BPF tone entirely Flight test data from the hardwall JT15D, with and without rods, obtained prior to the liner flight test are presented in Fig 4 The data are 100 Hz bandwidth narrowband sound pressure level spectra at the peak radiation angle of 40 deg from the inlet axis The spectrum without rods is generally broadband in nature No tone is evident near 4 00 kHz, which was the calculated BPF at a this fan speed of 8570 rpm This was expected since, according to Tyler Sofrin theory,[8] both rotor stator and rotor strut potential field interactions were acoustically cut off and rotor turbulence interactions were not significant in flight [2,3] In contrast, the spectrum with rods shows a dominant tone near 4 kHz This tone is believed to be due to an interaction between the 41 rods and the 28 fan blades to produce a (13,0) spinning mode Tyler Sofrin theory predicts a (13,0) mode at this frequency with no higher order radial modes present The tone level is nearly 20 dB above the broadband level It was thus decided that the primary design criterion would be to construct a liner to attenuate this dominant (13,0) acoustic mode by not more than 20 dB

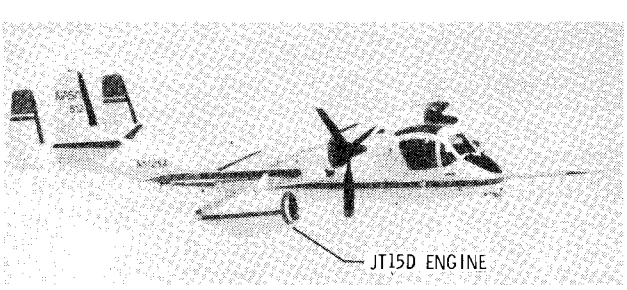

Fig 1 Modified OV 1B aircraft with JT15D turbofan engine

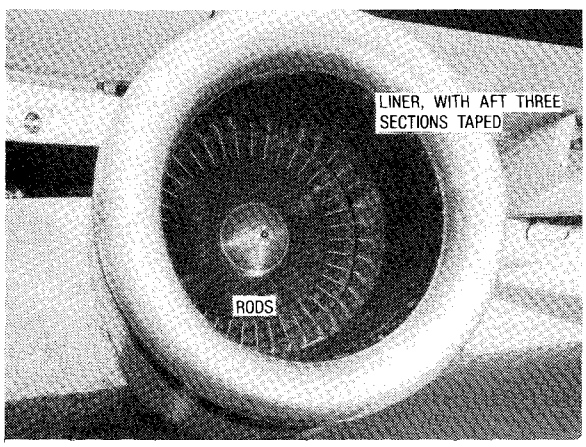

Fig 2 Modified JT15D inlet showing rods and liner installation

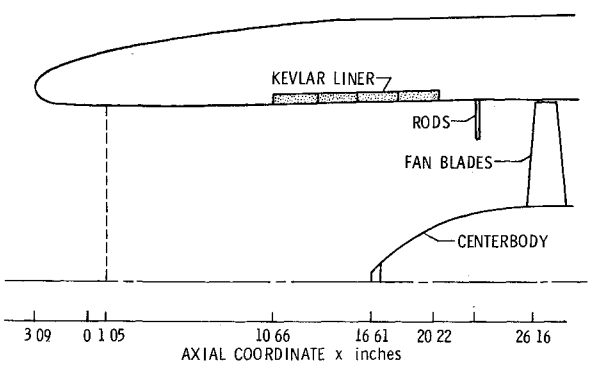

Fig 3 JT15D inlet geometry

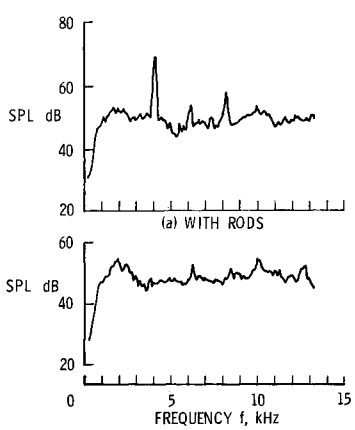

Fig 4 Far field hardwall SPL near peak radiation angle of 40 deg

Finite-Element Analysis

This section reviews the procedure by which the target design impedances for the liner were predicted

Fan Source Characteristics

Table 1 summarizes the fan source properties for the four target frequencies (3 73 4 00, 4 48 and 4 90 kHz) selected for liner design and flight-test verification In particular, the table lists for each test condition the cut off ratios calculated at the fan face for the (13,0), (13 1), and (13,2) spinning modes The fan section, it should be noted, is annular with inner and outer radii of about 4 05 and 10 5 in , respectively Reference to Table 1 reveals that at 3 73 kHz only the (13,0) spinning mode is cut on, that is $\xi > 1\ 0$ However, at 4 00 kHz the (13,1) mode is approaching cut on When the frequency is increased to 4 48 kHz, both the (13,0) and (13,1) spinning modes propagate and the source assumes a bimodal character, discounting near field cut off modes At a fan speed corresponding to 4 90 kHz the three lowest order $m = 13$ spinning modes are cut on Hence, of the four target liner design frequencies, 4 00 kHz is very close to the upper limit in terms of having a (13,0) spinning mode fan source

Cut off Ratio Analysis

The philosophy of the preliminary design stage was to obtain approximate liner impedance values at each of the four selected frequencies (Table 1) These approximate impedance values were based on Rice's cut off theory [9] A finite element computer model of the JT15D inlet was then utilized to adjust the liner impedance to compensate for the complexities of variable geometry, mean flow, and a (13,0) acoustic source distribution

Table 1 Fan source characteristics

Frequency kHz	Fan rpm	Mach No M_f	Cut off ratio ξ (13,0)	(13,1)	(13,2)
3 73	8 000	0 22	1 25	0 94	0 78
4 00	8 570	0 24	1 35	0 99	0 84
4 48	9 600	0 27	1 52	1 14	0 95
4 90	10,500	0 30	1 68	1 26	1 06

Table 2 Preliminary liner impedance based on cut off theory

Frequency kHz	ka	Impedance θ	χ
3 73	18 21	1 23	0 34
4 00	19 51	1 42	0 33
4 48	21 85	1 82	0 36
4 90	23 90	2 23	0 42

Rice's cut off ratio theory provides a correlation between the optimum liner impedance for a spinning mode (here $m = 13$) and its cut off ratio This approach as developed in Ref 9, is based on a single mode propagating in an infinitely long, acoustically lined duct The effects of flow therein are represented by a uniform plug flow with a 1/7th power law variation through the boundary layer

Table 2 summarizes the preliminary design liner impedance values as calculated using cut off ratio theory A uniform plug flow of M_f (see Table 1) with a nominal boundary layer thickness was assumed In the next design stage the preliminary liner impedance values were adjusted using a duct finite element computer program As will be seen, the predicted attenuation levels fall approximately in the 10 20 dB range, a desirable range for this design exercise

Finite Element Calculations

A finite element computer model of the JT15D inlet (Fig 3) was used to refine the preliminary design impedance values given in Table 2. Details of the finite element analysis are reported in Ref 4 Very briefly, linear isoparametic rec tangular elements are used in a Galerkin/weighted residual formulation Boundary conditions are satisfied by con straining the appropriate nodal variables The coefficient matrix of the resulting set of linear equations has a block tridiagonal form and a solution is achieved by LU decom position The discretization model used 400 elements axially and 20 elements radially

The finite element model covered the region extending axially from the source plane ($x = 26\ 16$) to the termination plane at the inlet's throat ($x = 1\ 05$) The source plane pressure distribution (boundary condition) was specified as the (13, 0) annular duct mode in accordance with the theory of Ref 10 At the termination plane a nonreflective impedance boundary condition was defined for the (13, 0) acoustic mode assuming a uniform flow distribution "[11] Radially the finite element model extended from the centerline or centerbody to the outer duct wall The sound absorbing properties of the duct liner were represented by a constant impedance A uniform quasi one dimensional plug flow was assumed and a sine roll off through the boundary layer was used to model the shear layer An average boundary layer thickness was assumed over the liner section

Table 3 summarizes, for the 4 00 kHz design condition the results of a sequence of calculations made by the finite element program The calculations begin with the liner im pedance ($\zeta = 1\ 42 + j0\ 33$) predicted by cut off ratio theory (Table 2) In terms of admittance, $\beta = 0\ 67 - j0\ 15$, where $\beta = 1/\zeta$ The imaginary component of β was held constant at $-0\ 15$ while the real part of β was varied as shown In this one dimensional search the attenuation peaked at about 18 5 dB for an impedance of about $\zeta = 2\ 19 + j0\ 82$ The real part of β was then held constant at $\beta_R = 0\ 40$ for a range of calculations made over β_I For this second one dimensional search the attenuation peaked at about 22 7 dB with an im pedance of $\zeta = 1\ 80 + j1\ 12$ This impedance ($\zeta = 1\ 80 + j1\ 12$) was taken as the target liner design impedance at 4 00 kHz

Table 3 Target liner impedance search, $f = 4\ 00$ kHz

β_R	$\zeta = [\beta_R - j0\ 15]^{-1}$	Attenuation dB	β_I	$\zeta = [0\ 40 - j\beta_I]^{-1}$	Attenuation dB
0 27		15 8	0 11		16 5
0 34		18 3	0 13		17 5
0 40	2 19 + j0 82	18 5	0 15	2 19 + j0 82	18 5
0 47		17 4	0 17		19 6
0 54		16 1	0 19		20 6
0 60		15 0	0 20		21 1
0 67	1 42 + j0 33	14 0	0 25	1 80 + j1 12	22 7
0 74		13 1	0 30		22 4
0.80		12.5	0.35		20.9

The off design point performance of this liner ($\zeta = 1\ 80 + j1\ 12$) was also checked At 3 73 kHz about 14 7 dB of attenuation was predicted by the finite element calculation For 4 48 and 4 90 kHz the attenuations were 10 5 and 8 2 dB, respectively It should be recalled from Table 1 that at 4 48 kHz the (13,1) radial acoustic mode is also cut on, whereas at 4 90 kHz both the (13 1) and (13,2) modes are cut on Thus, for frequencies above about 4 00 kHz it would be expected that a liner, designed on the basis of a (13,0) acoustic source would experience some degradation due to cut on and propagation of higher order radial modes In view of this it was decided to focus the design exercise on the 4 00 kHz design point and attempt to construct the liner such that the off design point performances would still be acceptable The liner design and fabrication details are discussed in the next section

Liner Impedance Implementation

In the previous section a liner target impedance was established This target impedance was implemented by means of the design procedure to be described in this section A summary of the geometry, and aeroacoustic and design parameters resulting from this procedure is given in Table 4

Liner Analysis

It was decided that a broadband or bulk absorber would be the appropriate acoustic element with which to achieve the desired liner performance characteristics Previous laboratory experience with a synthetic fiber (Kevlar 29) showed it to be satisfactory for achieving the desired design objective In addition a data base defining the acoustic propagation constant and characteristic impedance of Kevlar for the frequency range 0 50 3 50 kHz existed for modest bulk densities

Math Model

For a normal incidence acoustic wave the surface acoustic impedance ratio ζ of a bulk material of depth d terminated by a rigid surface is given by

$$\zeta = \zeta_c \coth \gamma d \tag{1}$$

where ζ_c and γ are the bulk material characteristic impedance ratio and propagation constant respectively Changes in bulk density will affect both ζ_c and γ, which will in turn affect ζ The essence of this design procedure was to judiciously choose ζ_c γ and d to drive ζ toward the desired target value Laboratory data (measured values of the bulk material characteristic impedance ratio ζ_c and propagation constant γ) were obtained for several different bulk densities These data taken over the limited frequency range of 0 5 to 3 5 kHz were compared with calculated values of ζ_c and γ using a math model developed by Hersh [7] General trends of ζ_c and γ were found to be adequately predicted by Hersh's model Fiber orientation constants which were not measured, were adjusted by trial to bring measured and calculated values of ζ_c and γ into relatively good agreement over the frequency range 0 5 3 5 kHz The model was then used as an aid to estimate ζ_c and γ for the test frequencies of interest given in Table 1 and for a range of attainable Kevlar bulk densities

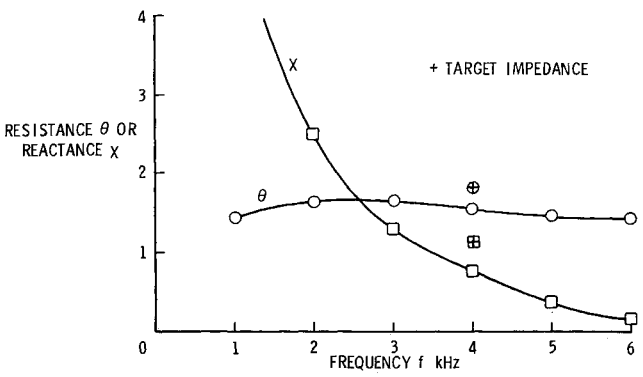

Fig 5 Kevlar liner impedance, $\zeta = \theta + j\chi$

Installation Effects

The installation of a bulk liner in an aircraft engine inlet duct requires a perforated face sheet to constrain the bulk material at the required density and to prevent flow erosion However depending upon hole geometry and porosity, the addition of a perforated face sheet can contribute a significant additional impedance This additional impedance arises from the intrinsic impedance ζ_f of the perforate, the interaction impedance between the perforate and bulk material ζ_i and a contribution ζ_n due to the effects of grazing flow and high sound pressure levels. The total installed impedance is then given by

$$\zeta = \zeta_c \coth \gamma d + \zeta_f + \zeta_i + \zeta_n \tag{2}$$

The philosophy adopted for this design application was to achieve the target impedance by means of the first term in Eq (2) and then minimize contributions from the remaining three terms In this manner uncertainties in the other components of ζ could be reduced This was accomplished by combining the math model for the bulk liner/cavity with math models describing the impedance contributions due to the perforate with grazing flow and high sound pressure levels [12 13]

The net result of this design procedure is shown in Fig 5 The figure shows the calculated components of normal incidence impedance of a bulk liner with a depth of 0 3 in and a density of 7 5 lbm/ft^3 retained by a 41% perforate and exposed to a Mach 0 2 grazing flow with a thin boundary layer Results are plotted down to 1 00 kHz because the math models were adjusted to fit the data in the frequency range 1 00 3 50 kHz as closely as possible The circles and squares denote calculated[12 13] resistance and reactance ratios respectively

Table 4 Liner design parameters

Overall geometrical dimensions	
Axial length	9 56 in (0 243 m)
Diameter (i d at fan face)	21 0 in (0 533 m)
Cavity depth	0 3 in (0 00762 m)
Cavity partition separation	
Circumferential	N/A
Axial	2 4 in (0 0610 m)
Perforate facesheet	
Material	304 S S
Thickness	0 03 in (0 000762 m)
Hole configuration	0 094 in (0 00238 m) staggered centers
Hole density	132 in^{-2} (2 05 × 10^6 m^{-2})
Hole diam	0 062 in (0 00157 m)
Porosity	41 0%
Bulk absorber	
Material	Kevlar 29
Bulk density (installed)	7 5 lbm/ft^3 (120 kg/m^3)
Fiber density	9 0 lbm/ft^3 (144 kg/m^3)
Fiber diameter	4 7 × 10^{-3} in (1 20 × 10^{-5} m)
Porosity	91 7%
Aeroacoustic parameters	
Mean flow Mach No	0 2
Boundary layer thickness	0 014 in (0 000356 m)
Sound pressure level (discrete)	145 dB
Air density	0 0755 lbm/ft^3 (1 21 kg/m^3)
Air temperature	21 C

The target values at 4 00 kHz are indicated in Fig 5 by the crossed symbols Note that both the resistance and reactance are less than the target values Either target component (resistance or reactance) alone could have been achieved at the cost of a greater target miss for the other component The interaction effect ζ_i decreased with increasing perforate porosity It was found to be negligible for a 41% perforate in contact with Kevlar at a density of 7.5 lbm/ft^3 This was established by measuring normal incidence impedance for several perforates of increasing porosity

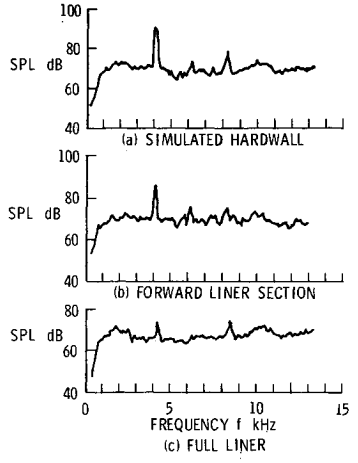

Fig 6 Far field SPL spectra near peak radiation angle of 40 deg

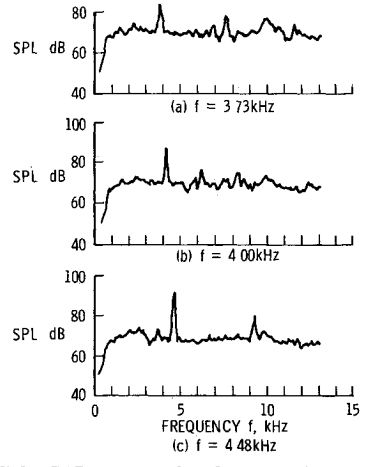

Fig 7 Far field SPL spectra for forward liner section near peak radiation angle of 40 deg

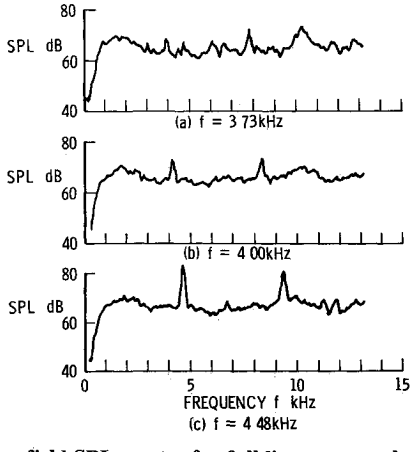

Fig 8 Far field SPL spectra for full liner near peak radiation angle of 40 deg

Extended Reaction

The finite element computer program assumed the liner to be locally reactive This requirement was approached by axially partitioning the liner into four equal 2 4 in sections and by packing the Kevlar to a high density (7 5 lbm/ft^3) For example, a Kevlar liner with this density has a phase speed ratio (relative to air) such that a ray incident at 45 deg on the Kevlar would penetrate at a refraction angle of about 25 deg with a spatial decay of 20 dB/in

Predicted Liner Performance

Table 5 summarizes the attenuations calculated by the finite element duct model using the liner impedances from Fig 5 At 4 00 kHz the design point impedance (Table 3) was $1\ 80+j1\ 12$ with an associated predicted attenuation of about 22 7 dB As can be seen from Table 5 the Kevlar liner used in the flight test exhibits an impedance of $1\ 550+j0\ 760$ The attenuation calculated by the finite element program is about 17 5 dB, which is still in the acceptable range of 10 20 dB of noise suppression

At 3 73 kHz the full liner produces a predicted attenuation of approximately 20 7 dB Similarly, the calculated at tenuation at 4 48 and 4 90 kHz are 9 6 and 5 9 dB, respec tively Calculated attenuations for just the forward liner section are also given in Table 5

Results and Discussion

In Fig 6 far field narrowband spectra are shown for three liner configurations The data are for a radiation angle, as measured from the duct centerline, of about 40 deg which is close to the peak radiation angle for the (13,0) spinning mode Figure 6a shows the spectrum for the hardwall inlet which was simulated by applying aluminum tape over the duct liner The BPF tone at 4 kHz peaks at about 20 dB above the broadband noise level As illustrated earlier with the aid of Fig 4a, this tone is believed to be entirely due to the (13,0) spinning mode generated by the interaction of the 41 rods with the 28 fan blades [1] The untaping of a single section (forward most section in Fig 3, $10\ 66 \le x \le 13\ 05$) results in a BPF tone level reduction of about 4 dB as shown in Fig 6b Uncovering the entire liner (Fig 3, $10\ 66 \le x \le 20\ 22$) results in about a 14 dB reduction (Fig 6c) Note also that the broadband level with the full liner exposed is several dB lower than for the simulated hardwall case Broadband noise reduction was an added benefit derived from this liner configuration

Liner effectiveness as a function of frequency is shown in Figs 7 and 8 The data are presented as narrowband sound pressure level (SPL) spectra recorded at a radiation angle of 40 deg for the nominal design frequencies of approximately 3.73, 4 00, and 4 48 kHz Data for the forward liner section (Fig 3 $10\ 66 < x < 13\ 05$) are shown in Fig 7 As frequency increases, the tone level at the BPF is seen to increase, in dicating that the liner is less effective with increasing frequency, i e , cut off ratio, as would be expected Similar results for the full liner are shown in Fig 8 It should be recalled that the liner was designed for a (13 0) spinning mode source Subsequent analysis[14] of the flight data reveals that the hardwall radiation pattern is totally dominated by the principal lobe for the (13,0) mode This is true even at the higher fan speeds where the higher order radial modes can propagate (Table 1) This implies relatively low amplitudes

Table 5 Predicted liner attenuations

Frequency kHz	ka	Impedance ζ θ	χ	Attenuation dB Full liner	Forward section
3 73	18 21	1 58	0 88	20 7	5 9
4 00	19 51	1 55	0 76	17 5	6 3
4 48	21 85	1 52	0 57	9 6	1 0
4.90	23.90	1.47	0.40	5.9	0.5

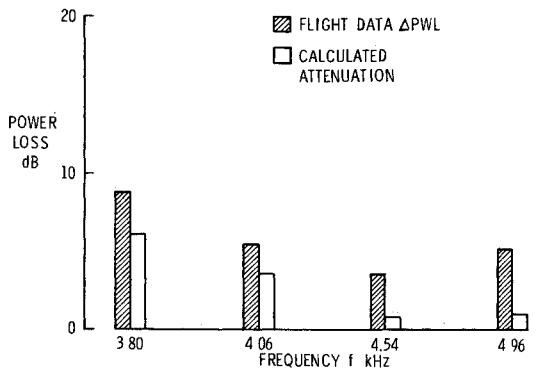

a) Forward liner section

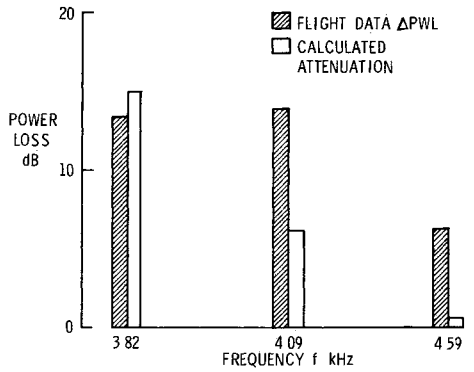

b) Forward two liner sections

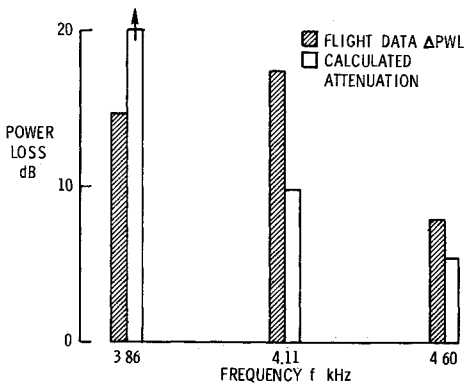

c) Forward three liner sections

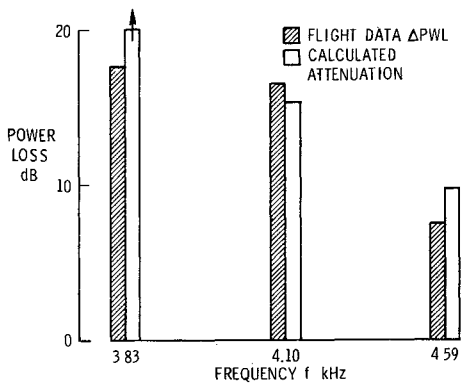

d) Full liner

Fig 9 Comparison of calculated liner attenuation with far field power loss

for the (13 1) and (13 2) spinning modes Thus designing the liner on the basis of a pure (13 0) spinning mode source ap pears valid

Figure 9 presents comparisons between calculated liner attenuation and measured far field power (insertion) loss for four liner length combinations The comparison of liner attenuation (transmission loss) with power insertion loss is valid, provided that the reflected waves generated at the liner entrance do not affect the acoustic source It is generally thought that the source mechanism is insensitive to such acoustic loading effects

The far field power loss was obtained by integrating the hardwall SPL and softwall liner SPL over the forward inlet hemisphere and taking the difference Data were first ad justed to a static equivalent, lossless atmospheric condition at a constant radius of 100 ft This adjustment for forward speed was achieved by compensating for the effects of retarded time, Doppler shift, and convective amplification Details of the entire data reduction procedures are discussed in Ref 3 Since hardwall and liner tests were conducted under different conditions, that is different days and/or different times on the same day, engine rpms were adjusted so that the free space BPF wave number k for corresponding runs were nominally the same Thus, it is observed that the frequencies shown in the various parts of Fig 9 differ slightly from the preliminary design values of 3 73, 4 00 4 48, and 4 90 kHz

An examination of Figs 9a c indicates that the calculated liner attenuations were generally less than the measured power losses An obvious exception is at 3 73 kHz where the predicted values are high; the vertical arrows in Figs 9c and 9d indicate off scale values This is not unexpected since at 3 73 kHz the cut off ratio (Table 1) for the (13 0) mode is about 1 25 Hence this mode is nearer cut on than at the other frequencies and unusually high attenuations are calculated

The calculated attenuations, for each liner length con figuration, follow the same trend of decreasing with in creasing frequency This is not the case for the measured power losses, as noted at 4 96 kHz for the forward liner section (Fig 9a) and 4 09 and 4 11 kHz for the two and three liner sections respectively (Figs 9b and 9c) The best agreement between measurement and calculation occurs for the full liner configuration (Fig 9d) where the differences are within about 2 dB for the 4 10 and 4 59 kHz cases

Concluding Remarks

This paper addressed the design, flight test and per formance evaluation of an engine inlet bulk acoustic liner Far field acoustic power (insertion) losses deduced from flight data were compared to in duct liner attenuations (trans mission losses) calculated by a finite element computer program These two liner performance indicators are generally equivalent, provided that reflections from the liner entrance do not change the acoustic source relative to the hardwall (without liner) configuration In some cases, as with the full liner configuration comparisons between flight deduced power loss and calculated in duct attenuation were within about 2 dB With the partial liner configurations, the agreement was not as good The calculated liner losses were generally less than the measured far field power losses

Several possible refinements can be advanced as having the potential to improve the agreement between measured and calculated liner power losses First a nonreflective ter mination impedance was used as a boundary condition in the finite element algorithm It would be preferable to couple a radiation model with the in duct finite element program so that calculated far field power losses could be directly compared with measured far field power loss data Second there were some cases where the finite element program exhibited numerical oscillations traceable to element mesh size in the boundary layer This is an area that will require future

work Third the duct liner local reaction assumption may have been only marginally satisfactory for the partial liner configurations

References

[1]Heidmann M F Saule A V , and McArdle J G Analysis of Radiation Patterns of Interaction Tones Generated by Inlet Rods in the JT15D Engine, AIAA Paper 79 0581 March 1979

[2]Preisser J S , Schoenster J A Golub R A and Horne C Unsteady Fan Blade Pressure and Acoustic Radiation from a JT15D 1 Turbofan Engine at Simulated Forward Speed AIAA Paper 81 0096 Jan 1981

[3]Preisser J S and Chestnutt, D 'Flight Effects on Fan Noise with Static and Wind Tunnel Comparisons AIAA Paper 83 0678 April 1983

[4]Abrahamson A L A Finite Element Algorithm for Sound Propagation in Axisymmetric Ducts Containing Compressible Mean Flow ' NASA CR 145209 June 1977

[5]Radecki K P and Johnstone, W H Bulk Absorber Inlet Treatment Investigation General Electric Co TM 75 151 1975

[6]Smith, C D and Parrott, T L An Experimental Study of the Effects of Water Repellant Treatment on the Acoustic Properties of Kevlar ' NASA TM 78654 Jan 1978

[7]Hersh A S and Walker B Acoustic Behavior of Fibrous Bulk Material AIAA Paper 80 0986 June 1980

[8]Tyler, J M and Sofrin T G Axial Flow Compressor Noise Studies ' *Transactions of SAE* Vol 70, 1962 pp 309 332

[9]Rice E J Optimum Wall Impedance for Spinning Modes—A Correlation with Mode Cut off Ratio *Journal of Aircraft* Vol 16 May 1979

[10]Zorumski, W E Acoustic Theory of Axisymmetric Multisectioned Ducts NASA TR R 419 1974

[11]Silcox R J and Lester, H C Sound Propagation Through a Variable Area Duct: Experiment and Theory *AIAA Journal* Vol 20, Oct 1982

[12]Eversman W Nelsen M D , Armstrong D , and Hall Jr , O J , Design of Acoustic Linings for Ducts with Flow *Journal of Aircraft* Vol 9 Aug 1972 pp 548 556

[13]Guess A W Calculation of Perforated Plate Liner Parameters from Specified Acoustic Resistance and Reactance *Journal of Sound and Vibration* Vol 40, Jan 1975 pp 119 137

[14]Preisser J S , Silcox, R J Eversman W and Parrett, A V A Flight Study of Tone Radiation Patterns Generated by Inlet Rods in a Small Turbofan Engine AIAA Paper 84 0499 Jan 1984